Effect of Nickel Promoter on Solvent-Free Sulphated Zirconia Catalyst for the Esterification of Acetic Acid with n-Butanol

by Hesti Wijayanti

EFFECT OF NICKEL PROMOTER ON SOLVENT-FREE SULPHATED ZIRCONIA CATALYST FOR THE ESTERIFICATION OF ACETIC ACID WITH N-BUTANOL

Hesti Wijayanti and Apinya Duangchan*

Department of Chemical Engineering, Faculty of Engineering, Kasetsart University, Bangkok, 10900, Thailand

A simple solvent-free preparation method was used to synthesize sulphated zirconia catalyst with various amounts of nickel promoter. This research investigated the effect of nickel addition to sulphated zirconia on the catalyst performance in esterification of acetic acid (a bio-oil model) with n-butanol. The results show that the addition of nickel contributed to the increase of sulphur content that bonded with nickel, the increase of thermal stability of the catalysts, and the formation of additional sulphate groups, and thus resulted in better catalytic performance compared to sulphated zirconia without nickel. More nickel being added resulted in a significant increase of acetic acid conversion; with 0.05 mol/mol nickel amount, the conversion was 97.93 %. This result represents a dramatic increase of about 2 and 3 times compared to the conversions of non-nickel sulphated zirconia catalyst and non-catalyst reactions, respectively.

Keywords: sulphated zirconia, nickel, esterification, acetic acid, n-butanol

INTRODUCTION

During the past decade, the shortage of fossil fuels and severity of environmental issues have led to a great interest in exploring renewable energy resources to enhance energy security and sustainability. As fossil fuels become exhausted, the development and utilization of renewable energy resources has attracted much attention.

Fast pyrolysis of biomass has been extensively investigated as a method for biomass conversion which results in pyrolysis oil (also known as bio-oil). However, bio-oil composition is very complex and contains a large amount of oxygenated compounds such as carboxylic acids, aldehydes, phenols, and ketones.[1] The high acid content of bio-oil, about 0.13 g/g (in palm-shell pyrolysis oil),[2] makes it highly acidic and corrosive,[3,4] which limits its applications as a fossil fuel substitute. The acids in bio-oil are also reactive and unstable at high temperatures, contributing to the acceleration of bio-oil aging and a decline in properties.[5] Consequently, upgrading processes to remove acids must be performed.

Catalytic esterification is widely studied for conversion of acids (i.e. formic acid, acetic acid, propionic acid) to their corresponding esters. Conventionally, esters are obtained from esterification in homogeneous conditions with liquid acid catalysts such as sulphuric, p-toluene sulphonic, or phosphoric acids.[6] As reported by Weerachanchai et al.,[2] using a sulphuric acid catalyst not only can give high acid conversion to esters, but also reduces the amount of active aldehydes in bio-oil. However, the use of these liquid catalysts results in some safety, economic, and environmental drawbacks such as toxicity, corrosivity, pollution, and separation of products. Therefore, replacing those acids with more environmentally-friendly solid acid catalysts is strongly favoured. Among strong acid catalysts, sulphated zirconia has attracted much attention since it exhibits promising catalytic activity in many reactions, such as hydrocarbon isomerization, methanol conversion to hydrocarbons, alkylation, acylation, esterification, etherification, condensation, nitration, and cyclization.[7] The weakness of sulphated zirconia is that it suffers from deactivation

due to coke formation at high temperatures, but this can be overcome by modifying it with various transition metals such as platinum.[7]

In recent years, much work has been done on studying the utilization of sulphated zirconia. However, so far, research using metals (i.e., Fe-Mn, Ni, Pt, Cr, Co, Al) on sulphated zirconia has only been applied in n-butane isomerization[8,9,10,11] and toluene disproportionation to produce benzene and xylenes.[12] Meanwhile, there has been little research published in which the work has used sulphated zirconia in bio-oil upgrading via esterification. Xu et al.[13] proposed that sulphated zirconia (SO_4^{2-}/ZrO_2) showed the best results compared to SO_4^{2-}/TiO_2 and SO_4^{2-}/SnO_2 through bio-oil reactive distillation by using ethanol. In addition, Tang et al.[14] and Dang et al.[15] promoted SO_4^{2-}/ZrO_2 with precious metals, Pd and Pt respectively, on SBA-15 support for upgrading bio-oil in supercritical ethanol under hydrogen pressure.

To the best of our knowledge, using nickel, a non-precious metal, over sulphated zirconia catalyst which is synthesized with a simple solvent-free method for esterification has not been investigated yet. This present work investigated the effect of adding nickel to sulphated zirconia and its catalytic activity for esterification of acetic acid with n-butanol. Acetic acid was selected as a model of the real bio-oil, since carboxylic acids contained in bio-oil typically include formic acid, acetic acid, propanoic acid, and low molecular unsaturated organic acids. Among them, formic and acetic acid account for about 80 % of the total acid amount.[16] Esterification is typically an endothermic reversible reaction. To drive the reaction forward, water removal is essential. In order to remove water, n-butanol

was used due to its higher boiling point compared to water, since it would stay in the solution while water was evaporated at reaction temperatures above its boiling point. Moreover, *n*-butanol is obtainable from renewable sources through fermentation processes.[17]

METHODOLOGY

Materials

The chemical materials, including acetic acid (CH_3COOH, 99.8 %, QReC), *n*-butanol ($C_4H_{10}OH$, 99.5 %, QReC, New Zealand), zirconium oxychloride ($ZrOCl_2 \cdot 8H_2O$, 99 %, QReC), ammonium sulphate (($NH_4)_2SO_4$, 99 %, Univar, Ajax Finechem, New Zealand), sodium hydroxide (NaOH, Univar, Ajax Finechem, New Zealand), nickel nitrate hexahydrate ($Ni(NO_3)_2.6H_2O$, 97 %QReC, New Zealand), and phenolphthalein (LobaChemie, Mumbai) were obtained from Roongsub Chemicals Company, Bangkok. All chemicals were used as received without further purification.

Catalyst Preparation

Sulphated zirconia catalysts were prepared by a solvent-free method previously described in Sun et al.[18] A 1:6 mole ratio of $ZrOCl_2 \cdot 8H_2O$ and $(NH_4)_2SO_4$ was ground in a porcelain mortar for 20 min at 30 °C (room temperature). Then it was placed in a crucible at this temperature for 18 h and calcined for 5 h at 600 °C. The synthesized catalyst is labelled SZ. This present work modified the previous preparation by addition of nickel to the SZ preparation. Amounts of 0.01, 0.03, and 0.05 mol/mol of nickel from $Ni(NO_3)_2.6H_2O$ were ground in addition to the 1:6 mole ratio of $ZrOCl_2 \cdot 8H_2O$ and $(NH_4)_2SO_4$ mentioned above to synthesize 0.01, 0.03, and 0.05 mol/mol nickel over sulphated zirconia catalysts. These catalysts are called 1Ni-SZ, 3Ni-SZ, and 5Ni-SZ, respectively, throughout this paper.

Catalyst Characterization

Nitrogen adsorption-desorption measurement

Nitrogen adsorption-desorption measurements were performed at −195.8 °C on a Quantachrome Autosorb-1C/MS instrument using a standard adsorption technique. Prior to measurement, the samples were outgassed at 200 °C for 15 h.

Scanning electron microscopy (SEM)

Scanning electron micrographs were obtained from a Philips XL 30 SEM with an energy dispersive X-ray of 13 kV and 10 000 × magnification. Prior to analysis, the sprinkled samples were coated with carbon as a conducting material using an Edwards Scancoat Six coating machine.

Transmission electron microscopy (TEM)

Transmission electron micrographs were recorded on a Hitachi transmission electron microscope HT 7700 operated at an accelerated voltage of 120 kV with 70 000 × magnification. All samples were first dispersed in alcohol and then a drop of the liquid was deposited on a copper grid coated with a formvar-carbon film.

X-ray fluorosence (XRF)

The chemical composition of the samples was determined using an X-ray analytical microscope Horiba Scientific XGT-5200 with 1000 mA current, XGT diameter of 10 μm, 200 s of live time, and X-ray tube voltage of 30 kV.

Infrared (IR) spectroscopy

The infrared spectra were recorded on a Tensor 27 Bruker FTIR spectrometer. The samples were prepared as thin films on KBr salt plates. The wave length used was 500–4000 cm^{-1} with a resolution of 4 cm^{-1}.

Thermogravimetric and derivative thermogravimetric analysis (TGA and DTG)

Thermogravimetric and derivative thermogravimetric analysis were carried out with a simultaneous DSC-TGA analyzer SDT 2960 Perkin Elmer instrument, in 40 mL/min of air flow, up to 1000 °C with a heating rate of 20 °C/min. The samples in the form of fine powder were placed in an alumina-covered crucible, and an empty crucible was used as a reference.

Catalytic Esterification

The esterification of acetic acid with *n*-butanol was carried out in a three-necked 250 mL Pyrex flask equipped with a magnetic stirrer, a reflux condenser, and a water separator (Dean-Stark apparatus), which was placed in a thermostatic oilbath. The reagent mixture (*n*-butanol and acetic acid with a mole ratio of 2.4:1, which was the optimum mole ratio from our preliminary study) was heated to 115 °C while being stirred at 750 rpm. Once the desired temperature was reached, the esterification reaction was started by introducing the catalyst in the form of 0.01 g/g solution (this value was fixed in this study as it exhibited the optimum condition for a similar reaction[19]). These conditions were maintained for 1 h. After the reaction was completed and the contents were cooled to 30 °C (room temperature), a 0.5 mL sample was taken and analyzed. The sodium hydroxide standard solution was used to measure the acetic acid conversion quantitatively using titration. Thus:

$$Acetic\ acid\ conversion\ =\ \left(1 - \frac{V}{V_0}\right) \times 100\% \qquad (1)$$

where V and V_0 are the volumes of standard sodium hydroxide solution consumed in neutralizing of 0.5 mL solution sample by changing the phenolphthalein to pink in the esterification process, and at the beginning of the reaction, respectively.

RESULTS AND DISCUSSION

Catalyst Characterization

Nitrogen adsorption-desorption measurement

According to the IUPAC classification, the typical type IV isotherm is characteristic of mesopore structures.[20] The shape of the isotherms in Figure 1 is typical of a type IV isotherm. The catalyst with the lowest nickel content (1Ni-SZ) exhibited hysteresis H3, as did that without the addition of nickel (SZ). Similar to SZ and 1Ni-SZ, the catalysts with medium (3Ni-SZ) and high (5Ni-SZ) nickel content also showed a H3 hysteresis loop. However, both of those catalysts demonstrated a wider pore size distribution (1–30 nm) compared to that of SZ (4–30 nm), indicating the existence of microporosity,[20] and in the case of 5Ni-SZ, the microporosity can be even more clearly observed (see inset to Figure 1d).

The BET surface area was reduced in the order of SZ > 1Ni-SZ > 3Ni-SZ > 5Ni-SZ (Table 1). In comparison with SZ, the declines of surface area were about 3, 9, and 20 times for 1Ni-SZ, 3Ni-SZ, and 5Ni-SZ, respectively. This result was also confirmed by the reduction of support (ZrO_2) composition that
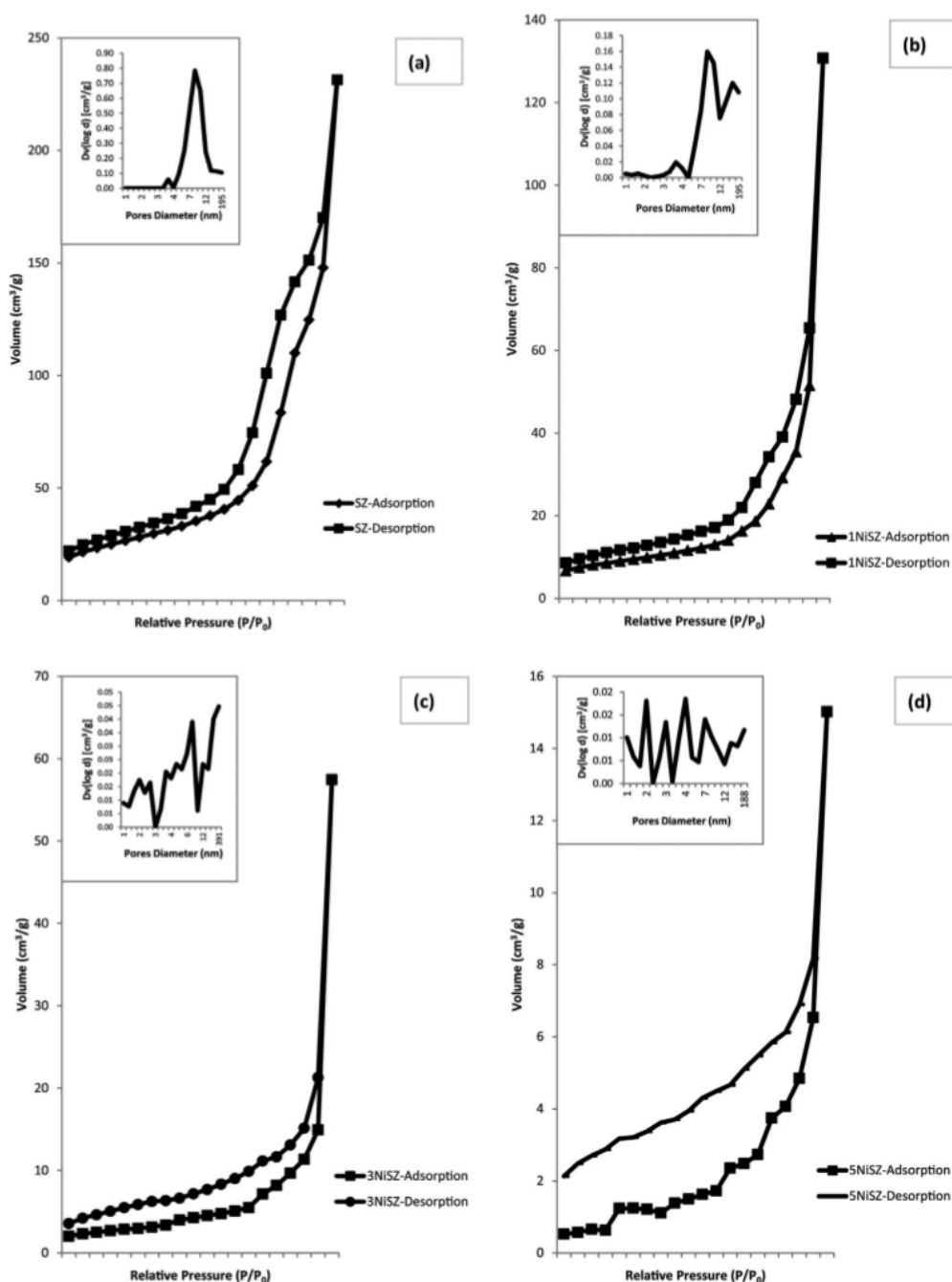
Figure 1. Adsorption-desorption isotherm and BJH pore distribution of catalysts: (a) SZ, (b) 1Ni-SZ, (c) 3Ni-SZ, (d) 5Ni-SZ.

rose as the nickel content increased, indicating that the added nickel was mainly located inside the mesoporous channel.[21] Similar to the surface area trend, both the pore volume and the pore diameter were significantly reduced (Table 1). These could be attributed to two possibilities: the decrease of distribution of mesoporous sulphated zirconia in the catalysts due to the high loading of the metal active component, and/or the blocking of mesopores because of the incorporation of nickel particles.[22,23]

SEM

Figure 2 shows the surface morphology of the synthesized catalysts. Without nickel addition, the surface of SZ catalyst shows a clean and smooth surface with small and large agglomerations on the support (Figure 2a). The addition of nickel during SZ synthesis leads to cracking of the support. The more nickel added in the preparation, the more cracking on the support

Table 1. Physical properties of the prepared catalysts

Catalyst	BET surface area (m²/g)	Pore volume (cm³/g)	Pore diameter (nm)[a]	Composition (g/100g, mass%)[b]		
				NiO	SO₃	ZrO₂
SZ	86.87	0.358	7.786	-	0.008	99.992
1Ni-SZ	29.06	0.202	7.770	1.714	0.036	98.249
3Ni-SZ	9.23	0.089	2.177	4.572	0.040	95.388
5Ni-SZ	4.34	0.023	2.182	8.576	0.043	91.381

[a]Based on BJH desorption method
[b]XRF results

was formed (Figures 2 b–d), as well as the more nickel filled the pores. As a result, the pore diameter and the pore volume of supports decreased with the increase of nickel addition.These results were consistent with the physical properties obtained from nitrogen adsorption-desorption measurements mentioned above.

TEM

TEM images of the SZ and 5Ni-SZ appear in Figure 3. The SZ showed irregular shapes of nanosize particles which were highly aggregated (Figure 3a). On the other hand, Figure 3b demonstrates that with the 0.05 mol/mol nickel addition, the 5Ni-SZ image presented smaller sizes of particles (on average ∼10 nm) and also moderate agglomeration (in accordance with the SEM result).

XRF

XRF results confirmed that calcination at 600 °C caused some ion sulphates to be decomposed to form SO_3 (in agreement with TGA result described below). Ion sulphate can be decomposed to SO_3 at high calcination temperatures.[24] Furthermore, the formed SO_3 increased with the addition of nickel. Nickel bonds with sulphate. As more nickel was added, more sulphates were bonded; as a result, the formed SO_3 increased with the increase of nickel content (Table 1).

IR-spectroscopy

The IR spectra of the sulphated zirconia catalysts containing different amounts of nickel, and also without nickel, are shown in
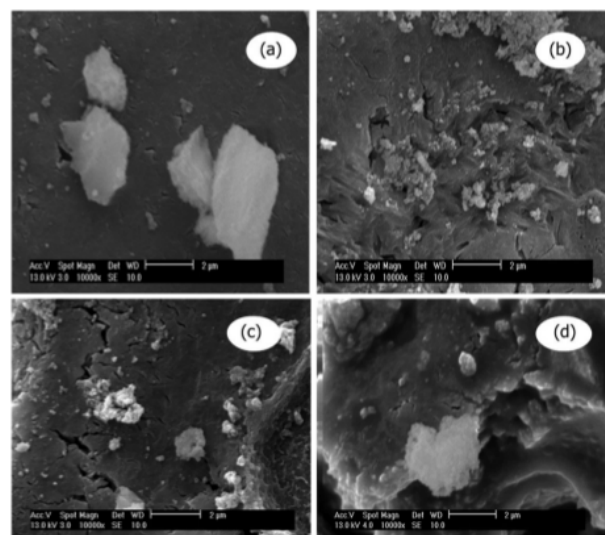
Figure 4. All of the spectra possessed a broad peak at around $3450\,cm^{-1}$, attributed to the vibration of hydroxyl groups.[25,26] The other similar peaks are near $2370\,cm^{-1}$, corresponding to organic residue from the precursors,[26] and an intense peak near $1650\,cm^{-1}$ due to the characteristic of non-dissociated water molecules (δ_{HOH}).[26] From previous work, it is known that the IR bands of the sulphate groups are in the region of 900–$1200\,cm^{-1}$.[27] This work demonstrated that, in addition to two peaks at about $1250\,cm^{-1}$ and $1160\,cm^{-1}$ as observed for SZ, Ni-SZ catalysts demonstrated two additional peaks of sulphate groups at about $1060\,cm^{-1}$ and $1010\,cm^{-1}$. This implies that nickel addition during preparation of sulphated zirconia possibly contributes to the formation of more sulphate group bonds, as observed for 1Ni-SZ, 3Ni-SZ, and 5Ni-SZ (in agreement with the TGA-DTG results described below).

Furthermore, the effect of nickel amount can be seen in the IR spectra. As the amount of nickel increased, the peaks became narrower, which implies an increase in the sulphate amount. This result suggests that a situation with nickel added to sulphated zirconia catalyst is able to retain more sulphur than a situation without nickel due to the addition of the structure of sulphate groups in sulphated zirconia, which is consistent with the work of Wang et al.[28] on using alumina with sulphated zirconia. The next peaks different from those of SZ were observed for Ni-SZ at $670\,cm^{-1}$, which is characteristic of Ni-O stretching vibration mode.[29] The other peaks obtained for all prepared catalysts were at around $770\,cm^{-1}$ and $620\,cm^{-1}$, and these correspond to the characteristics of ZrO_2.[30]

TGA and DTG

The results of thermal analysis of the prepared catalysts are presented in Figure 5. The highest mass loss is shown by the catalyst with the highest nickel content (5Ni-SZ). The order of the

Figure 2. SEM images of prepared catalysts: (a) SZ, (b) 1Ni-SZ, (c) 3Ni-SZ, (d) 5Ni-SZ.
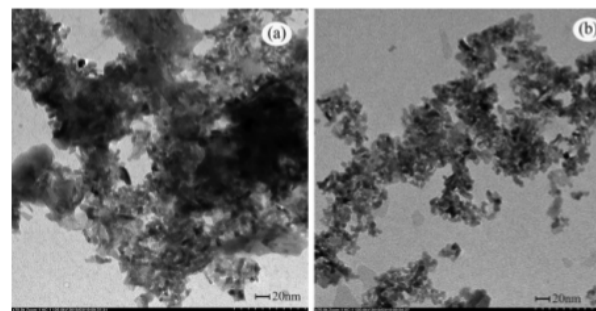
Figure 3. TEM images of prepared catalysts (70 000 × magnification): (a) SZ, (b) 5Ni-SZ.
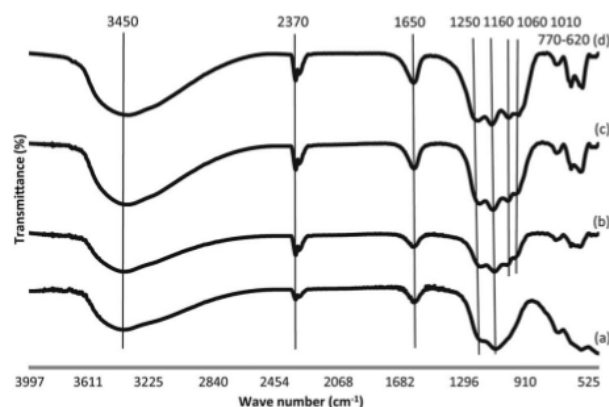
Figure 4. IR spectra of prepared catalysts: (a) SZ, (b) 1Ni-SZ, (c) 3Ni-SZ, (d) 5Ni-SZ.
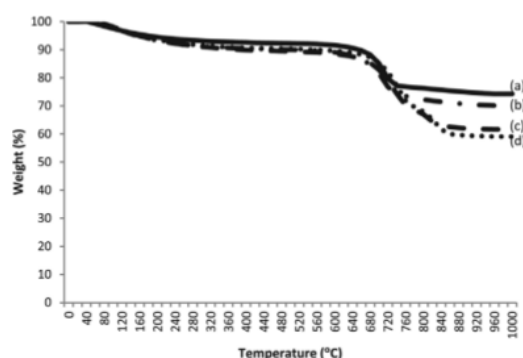
Figure 5. TGA curves of prepared catalysts: (a) SZ, (b) 1Ni-SZ, (c) 3Ni-SZ, (d) 5Ni-SZ.

decomposed amount of sulphate is SZ < 1Ni-SZ < 3Ni-SZ < 5Ni-SZ. This suggests that the sulphur content of those catalysts is in the same order.

Table 2 shows the mass losses during heating from 30–1000 °C in air flow. The first region was due to the loss of water and also the components of the precursors; this mass loss was continuous until about 500 °C, but with a decreasing rate.[31,32,33] Srinivasan et al.[34] and Sun et al.[18] also observed similar regions for sulphated zirconia heated in air, occurring first between 100–500 °C and then above 500 °C, the latter of which corresponds to sulphate decomposition. Interestingly, in this work, besides the second region, which showed an increase as the amount of nickel

rose, a third region with similar trends as those found in the second region was also detected for Ni-SZ catalysts.

From the DTG curves (Figure 6), it can be seen that all catalysts show similar peaks occurring around 100–500 °C. These first peaks were due to water loss and the decomposition of the precursors, as mentioned above when discussing the TGA results.[32,33] These second peaks were observed at 710, 710, 730, and 740 °C for SZ, 1Ni-SZ, 3Ni-SZ, and 5Ni-SZ, respectively – similar to results in the work of Jyothi et al.,[23] who observed the decomposition of sulphate in sulphated zirconia at 700–750 °C. These results indicated that the decomposition temperature increased by increasing the nickel content as well as the mass loss (in agreement with the TGA results).

Consistently with previous research,[35] the increase in sulphate loading shifted peak maxima towards the high temperature region. Moreover, in contrast to there being only one sulphate decomposition peak, as observed for the SZ catalyst, Ni-SZ catalysts demonstrated additional sulphate decomposition peaks at 780, 820, and 840 °C for 1Ni-SZ, 3Ni-SZ, and 5Ni-SZ, respectively, showing the presence of sulphate groups with different thermal stability.[36] These results imply that the addition of nickel might contribute to the rise of sulphur decomposition temperature, as suggested by Srinivasan et al.[34] and Wang et al.[28] that the effects of platinum and alumina on sulphated zirconia catalyst were an increase of sulphur retention, and thus the density of acid sites.

Catalytic Esterification

The effect of nickel addition to sulphated zirconia catalytic activity in esterification of acetic acid with *n*-butanol is shown in Figure 7. It shows the conversion obtained from different nickel content catalysts. For comparison, the conversion of SZ in the absence of nickel and for the esterification reaction without catalyst are also presented.

The acetic acid conversions after esterification at 115 °C for 1 h with a mole ratio of *n*-butanol to acetic acid of 2.4:1 and with catalyst loading of 0.01 g/g mixed solution were 72.52 %, 74.94 %, 95.58 %, and 97.93 % for SZ, 1Ni-SZ, 3Ni-SZ, and 5Ni-SZ, respectively. For comparison, without catalyst, the conversion obtained was only 31.33 %; it increased by more than twice when using SZ. Furthermore, the addition of a small amount of nickel in sulphated zirconia preparation (1Ni-SZ) only slightly increased the conversion compared to SZ, indicating that adding a small amount of nickel has little effect on the catalytic activity of sulphated zirconia under these conditions. However, as more nickel was added, the conversion dramatically increased to about 3 times higher than the results without catalyst (as observed for 5Ni-SZ).

As esterification is an acid-catalyzed reaction, the rise of conversion with the increase of nickel is possibly due to the increase of sulphur content that bonded with nickel (supported by TGA-DTG and XRF results), the increase of thermal stability of Ni-

Table 2. Mass loss of the prepared catalysts as resulted from TGA curves

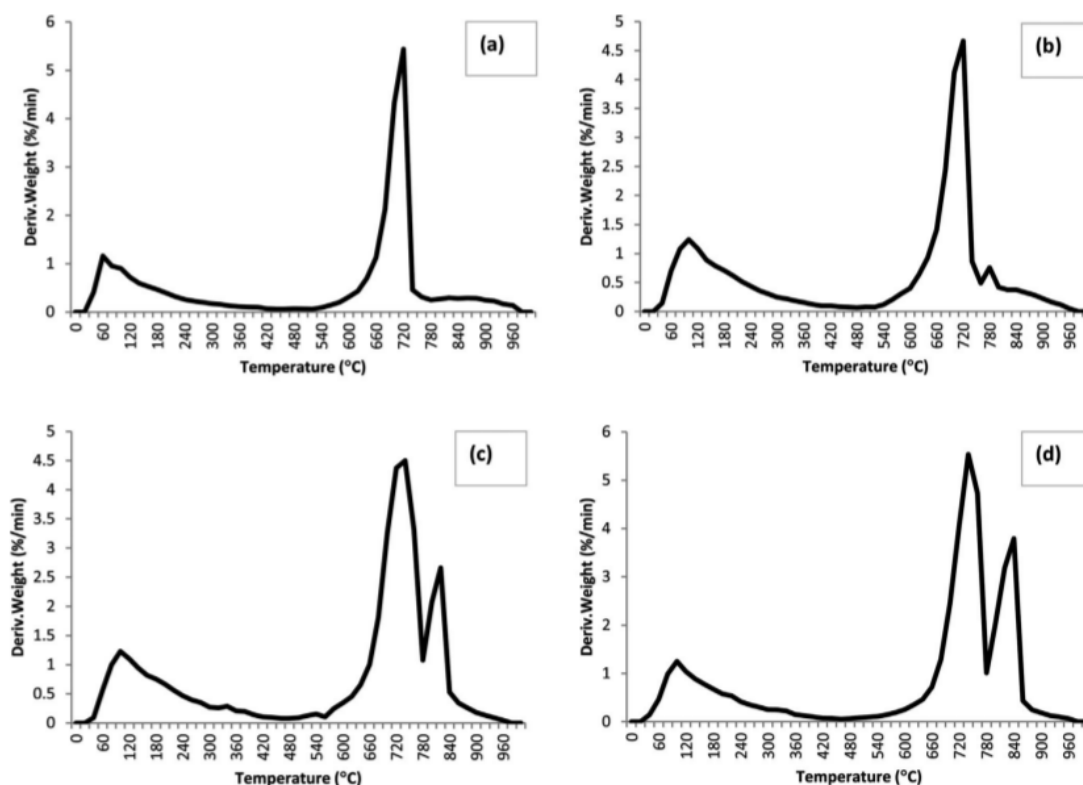|	SZ		1Ni-SZ		3Ni-SZ		5Ni-SZ	
	Range (°C)	mass% loss	Range (°C)	mass% loss	Range (°C)	mass% loss	Range (°C)	mass% loss
Region-1	60–500	6.33	100–500	7.30	100–500	8.30	100–500	7.37
Region-2	570–750	14.95	560–760	16.25	570–760	18.85	590–780	20.18
Region-3	-	-	760–810	1.44	760–900	8.10	780–900	10.09

Figure 6. DTG curves of prepared catalysts: (a) SZ, (b) 1Ni-SZ, (c) 3Ni-SZ, (d) 5Ni-SZ.

SZ catalysts, and the formation of more sulphate groups compared to those of SZ (supported by FTIR results). Yamaguchi[27] reported that the IR bands of the sulphate groups in the region of 900–1200 cm^{-1} exhibited high catalytic activity. Moreover, nickel incorporation also resulted in the formation of additional acid sites on the ZrO_2 support.[22] In addition, Adeeva et al.[37] suggested that the extraordinary activity of metal-modified sulphated ZrO_2 is likely due to a good stabilization of the surface intermediates. As the result, the Ni-SZ catalysts prepared in this work exhibited better catalytic performances than that of SZ catalyst.

The catalyst prepared in this work (5Ni-SZ) showed results comparable to those of previous research on esterification of acetic acid and n-butanol. Results for various catalysts are presented in Table 3.
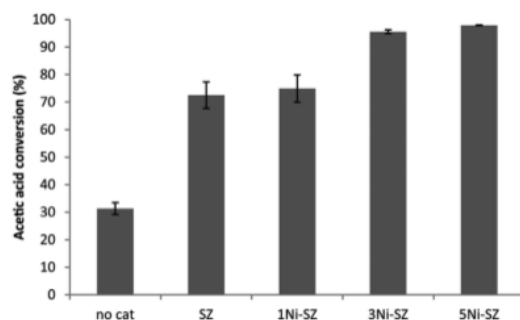

Figure 7. Catalytic activity of prepared catalysts. Reaction conditions: 115 °C for 1 h with a mole ratio of n-butanol to acetic acid of 2.4:1 and with catalyst loading of 0.01 g/g mixed solution.

Catalyst Stability

Many solid acid catalysts lose their catalytic activities in water-containing solutions due to severe poisoning of the acid sites by water.[43] To investigate the stability of the prepared catalyst, the used 5Ni-SZ (which showed the highest catalytic activity in the present study) from the first cycle of the reaction was separated via decantation, vaporized to remove the liquid, and dried at 120 °C for 1h before being reused in the next run under the same reaction conditions. The results obtained are presented in Figure 8.

From these results, it can be concluded that the 5Ni-SZ showed high stability for the first 3 cycles with the acid conversion of both the 2nd and 3rd cycles being close to that of the 1st cycle (fresh 5Ni-SZ); the values obtained were 97.75 % and 96.81 % for the 2nd and 3rd cycles, respectively. Unfortunately, the conversion decreased to 90.81 % by the 4th cycle, and in the 5th was reduced by about 20 % with respect to the fresh one. However, even this result was about 5 % greater than the conversion obtained with fresh 1Ni-SZ.

CONCLUSIONS

A simple solvent-free preparation method was applied to synthesize sulphated zirconia catalysts with a nickel promoter. The addition of nickel increased the sulphur content that bonded with nickel, the thermal stability of Ni-SZ catalysts, and the number of sulphate groups compared to SZ. The nickel addition resulted in better catalytic performance compared to sulphated zirconia without nickel. More nickel being added resulted in a significant increase in acetic acid conversion. The catalytic activity of prepared catalysts for esterification of acetic acid and n-butanol under the present conditions decreases in the following order: 5Ni-

Table 3. Results of esterification of acetic acid and n-butanol in a batch reaction with various catalysts

No.	Catalyst	Conditions	Conversion (%)
1.	20% TPA/AT-GMB (Dodecatungstophosphoric acid on acid activated bentonite; Bhorodwaj and Dutta[38])	150 °C; 0.3 g catalyst; mole ratio of acid:alcohol 3:1; 12 h	88
2.	ZAH-TA-MPA15 (Molybdophosphoric acid intercalated zinc-aluminium HTlc-terephtalate; Das and Parida[39])	98 °C; 0.025 g catalyst; mole ratio of acid:alcohol 1:16; 4 h	84.15
3.	Water washed-manganese nodule leached residue (MNLR; Dash and Parida[40])	98 °C; 0.025 g catalyst; mole ratio of acid:alcohol 1:16; 4 h	76.6
4.	Molybdena-vanadia supported on alumina (Mitran et al.[19])	100 °C; catalyst loading 1 mass% of mixture solution; mole ratio of acid:alcohol 1:3; 3 h	85
5.	Amberlyst-15 (Toor et al.[41])	93 °C; 13.96 g catalyst; mole ratio of acid:alcohol 1:5; 2 h	95
6.	V/γAl$_2$O$_3$ (Mitran et al.[42])	100 °C; catalyst loading 0.7 mass% of mixture solution; mole ratio of acid:alcohol 1:1; 4 h	81
7.	5Ni-SZ (present study)	115 °C; catalyst loading 1 mass% of mixture solution; mole ratio of acid:alcohol 1:2.4; 1 h	97.93
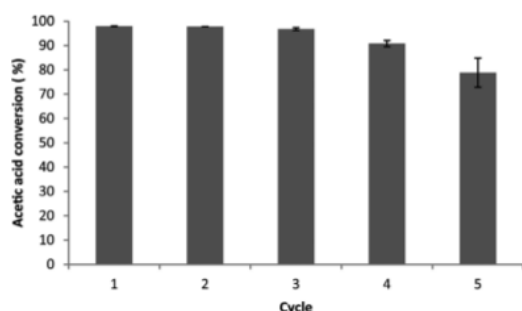
Figure 8. Reusability of prepared catalysts. Reaction conditions: 115 °C for 1 h with a mole ratio of n-butanol to acetic acid of 2.4:1 and with catalyst loading of 0.01 g/g mixed solution.

SZ > 3Ni-SZ > 1Ni-SZ > SZ. The 5Ni-SZ catalyst also showed high stability under repeated use for three cycles under the present study conditions.

ACKNOWLEDGEMENTS

REFERENCES

[1] W. Li, C. Pan, L. Sheng, Z. Liu, P. Chen, H. Lou, X. Zheng, *Bioresour. Technol.* **2011**, *102*, 9223.

[2] P. Weerachanchai, C. Tangsathitkulchai, M. Tangsathitkulchai, *Korean J. Chem. Eng.* **2012**, *29*, 182.

[3] J. Peng, P. Chen, H. Lou, X. Zheng, *Energ. Fuel.* **2008**, *22*, 3489.

[4] Z. Tang, Q. Lu, Y. Zhang, X. Zhu, Q. Guo, *Ind. Eng. Chem. Res.* **2009**, *48*, 6923.

[5] X. Li, R. Gunawan, Y. Wang, W. Chaiwat, X. Hu, M. Gholizadeh, D. Mourant, J. Bromly, C. Z. Li, *Fuel* **2014**, *116*, 642.

[6] E. Lotero, Y. Liu, D. E. Lopez, K. Suwannakarn, D. A. Bruce, J. G. Goodwin Jr., *Ind. Eng. Chem. Res.* **2005**, *44*, 5353.

[7] G. D. Yadav, J. J. Nair, *Micropor. Mesopor. Mat.* **1999**, *33*, 1.

[8] E. A. Garcia, E. H. Rueda, A. J. Rouco, *Appl. Catal. A-Gen.* **2001**, *210*, 363.

[9] D. J. Mcintosh, R. A. Kydd, J. M. Hill, *Chem. Eng. Commun.* **2004**, *191*, 137.

[10] J. H. Wang, C. Y. Mou, *Catal. Today* **2008**, *131*, 162.

[11] M. A. Coelho, D. E. Resasco, E. C. Sikabwe, R. L. White, *Catal. Lett.* **1995**, *32*, 253.

[12] A. L. C. Pereira, S. G. Marchetti, A. Albornoz, P. Reyes, M. Oportus, M. C. Rangel, *Appl. Catal. A-Gen.* **2008**, *334*, 187.

[13] J. Xu, J. Jiang, Y. Sun, Y. Lu, *Biomass Bioenerg.* **2008**, *32*, 1056.

[14] Z. Tang, Q. Lu, Y. Zhang, X. Zhu, Q. Guo, *Ind. Eng. Chem. Res.* **2009**, *48*, 6923.

[15] Q. Dang, Z. Luo, J. Zhang, J. Wang, W. Chen, Y. Yang, *Fuel* **2013**, *103*, 683.

[16] H. Cui, C. Ma, Z. Li, W. Yi, *Fuel Chem. Technol.* **2011**, *39*, 347.

[17] T. C. Ezeji, N. Qureshi, H. P. Blaschek, *J. Biotechnol.* **2005**, *115*, 179.

[18] Y. Sun, S. Ma, Y. Du, L. Yuan, S. Wang, J. Yang, F. Deng, F. Xiao, *J. Phys. Chem. B* **2005**, *109*, 2567.

[19] G. Mitran, O. D. Pavel, I. C. Marcu, *J. Mol. Catal. A-Chem.* **2013**, *370*, 104.

[20] K. S. W. Sing, D. H. Everett, R. A. W. Haul, L. Moscou, R. A. Pierotti, J. Rouquerol, T. Siemieniewska, *Pure Appl. Chem.* **1985**, *57*, 603.

[21] S. Garg, K. Soni, G. M. Kumaran, R. Bal, K. Gora-Marek, J. K. Gupta, L. D. Sharma, G. M. Dhar, *Catal. Today* **2009**, *141*, 125.

[22] Y. Yang, C. Ochoa-Hernandez, V. A. P. O'Shea, P. Pizarro, J. M. Coronado, D. P. Serrano, *Appl. Catal. B-Env.* **2014**, *145*, 91.

[23] T. M. Jyothi, K. Sreekumar, M. B. Talawar, S. P. Mirajkar, B. S. Rao, S. Sugunan, *Polish J. Chem.* **2000**, *74*, 801.

[24] B. R. Vahid, N. Saghatoleslami, H. Nayebzadeh, A. Maskooki. *Chem. Biochem. Eng. Q.* **2012**, *26*, 71.

[25] M. Signoretto, F. Pinna, G. Strukul, P. Chies, G. Cerrato, S. D. Ciero, C. Morterra, *J. Catal.* **1997**, *167*, 522.

[26] F. Babou, G. Coudurier, J. C. Vedrine, *J. Catal.* **1995**, *152*, 341.

[27] T. Yamaguchi, *Appl. Catal.* **1990**, *61*, 1.

[28] J. H. Wang, C. Y. Mou, *Catal. Today* **2008**, *131*, 162.

[29] H. Qiao, Z. Wei, H. Yang, L. Zhu, X. Yan, *J. Nanomater.* **2009**, DOI: 10.1155/2009/795928.

[30] N. Kamoun, M. K. Younes, A. Ghorbel, A. S. Mamede, *Ionics* **2015**, *21*, 221.

[31] S. Chokkaram, R. Srinivasan, D. R. Milburn, B. H. Davis, *J. Colloid Interf. Sci.* **1994**, *165*, 160.

[32] M. A. A. Elmasry, A. Gaber, E. M. H. Khater, *J. Therm. Anal.* **1998**, *52*, 489.

[33] W. Brockner, C. Ehrhardt, M. Gjikaj, *Thermochim. Acta* **2007**, *456*, 64.

[34] R. Srinivasan, R. A. Keogh, D. R. Milburn, B. H. Davis, *J. Catal.* **1995**, *153*, 123.

[35] F. H. Alhassan, U. Rashid, M. S. Al-Qubaisi, *Powder Technol.* **2014**, *253*, 809.

[36] J. R. Sohn, W. C. Park, *Korean J. Chem. Eng.* **2002**, *19*, 580.

[37] V. Adeeva, J. W. de Haan, J. Janchen, G.D. Lei, V. Schunemann, L. J. M. van de Ven, W. M. H. Sachtler, R. A. van Santen, *J. Catal.* **1995**, *151*, 364.

[38] S. K. Bhorodwaj, D. K. Dutta, *Appl. Clay Sci.* **2011**, *53*, 347.

[39] J. Das, K. M. Parida, *J. Mol. Catal. A-Chem.* **2007**, *264*, 248.

[40] S. S. Dash, K. M. Parida, *J. Mol. Catal. A-Chem.* **2007**, *266*, 88.

[41] A. P. Toor, M. Sharma, G. Kumar, R. K. Wanchoo, *BCREC* **2011**, *6*, 23.

[42] G. Mitran, E. Mako, A. Redey, I. C. Marcu, *C. R. Chim.* **2012**, *15*, 793.

[43] L. Zhou, B. Xu, W. Hua, Y. Yue, Z. Gao, *Catal. Commun.* **2008**, *9*, 2274.

Effect of Nickel Promoter on Solvent-Free Sulphated Zirconia Catalyst for the Esterification of Acetic Acid with n-Butanol

| Exclude quotes | Off | | Exclude matches | Off |
| Exclude bibliography | On | | | |